Link sito dell'editore: https://www.sciencedirect.com/science/article/abs/pii/S1549963418301102

Link codice DOI: https://doi.org/10.1016/j.nano.2018.05.018

Citazione bibliografica dell'articolo:

Vergara D, Bianco M, Pagano R, Priore P, Lunetti P, Guerra F, Bettini S, Carallo S, Zizzari A, Pitotti E, Giotta L, Capobianco L, Bucci C, Valli L, Maffia M, Arima V, Gaballo A. An SPR based immunoassay for the sensitive detection of the soluble epithelial marker E-cadherin. Nanomedicine. 2018, 14(7):1963-1971.

An SPR based immunoassay for the sensitive detection of the soluble epithelial marker E-cadherin

Daniele Vergara, PhD[a,b,*,1], Monica Bianco, PhD[c,1], Rosanna Pagano, PhD[a], Paola Priore, PhD[c], Paola Lunetti, PhD[a], Flora Guerra, PhD[a], Simona Bettini, PhD[d], Sonia Carallo, AS[c], Alessandra Zizzari, PhD[c], Elena Pitotti, BS[b], Livia Giotta, PhD[a], Loredana Capobianco, PhD[a], Cecilia Bucci, PhD[a], Ludovico Valli, PhD[a], Michele Maffia, PhD[a,b], Valentina Arima, PhD[c], Antonio Gaballo, PhD[c,**]

[a]*Department of Biological and Environmental Sciences and Technologies, University of Salento, Lecce, Italy*
[b]*Laboratory of Clinical Proteomic, "Giovanni Paolo II" Hospital, ASL-, Lecce, Italy*
[c]*CNR-NANOTEC, Institute of Nanotechnology c/o Campus Ecotekne, University of Salento, Lecce, Italy*
[d]*Department of Innovation Engineering, University of Salento, Lecce, Italy*

Received 28 February 2018; accepted 28 May 2018

Abstract

Protein biomarkers are important diagnostic tools for cancer and several other diseases. To be validated in a clinical context, a biomarker should satisfy some requirements including the ability to provide reliable information on a pathological state by measuring its expression levels. In parallel, the development of an approach capable of detecting biomarkers with high sensitivity and specificity would be ideally suited for clinical applications. Here, we performed an immune-based label free assay using Surface Plasmon Resonance (SPR)-based detection of the soluble form of E-cadherin, a cell–cell contact protein that is involved in the maintaining of tissue integrity. With this approach, we obtained a specific and quantitative detection of E-cadherin from a few hundred microliters of serum of breast cancer patients by obtaining a 10-fold enhancement in the detection limit over a traditional colorimetric ELISA.

Key words: E-cadherin; Breast cancer; Surface plasmon resonance; Quartz crystal microbalance with dissipation monitoring; Epithelial mesenchymal transition

The epithelial protein E-cadherin (Ecad, *CDH1* gene) is a single pass transmembrane glycoprotein that plays a role in tissue organization by regulating cell contact formation and cell polarity.[1] E-cadherin is a member of the classic type I cadherin family and a major constituent of adherents junctions (AJs). *CDH1* gene codifies for a protein of 120 kDa that is constituted by five extracellular calcium-binding repeats, a single transmembrane region, and a cytoplasmic domain that interacts with a range of proteins including catenins, and the underlying cytoskeleton, regulating several intracellular signal transduction pathways.[1]

Conflict of interest: The authors declare no commercial associations, current and within the past five years, that might pose a potential, perceived or real conflict of interest.

Disclosures: We gratefully acknowledge funding from the Apulia Regional Cluster project "SISTEMA" project code T7WGSJ3. We thank ISBEM and Hospital Giovanni Paolo II clinicians for their help with human samples collection. This research was also supported by "FutureInResearch" APQ Ricerca Regione Puglia. This work was also partially supported by AIRC (Associazione Italiana per la Ricerca sul Cancro), Investigator Grant 2016 N. 19068 to C. B.

*Correspondence to: D. Vergara, Department of Biological and Environmental Sciences and Technologies, University of Salento, Via per Arnesano, 73100 Lecce, Italy.

**Correspondence to: A. Gaballo, CNR-NANOTEC, Institute of Nanotechnology c/o Campus Ecotekne, University of Salento, Via per Arnesano, 73100 Lecce, Italy.

E-mail addresses: daniele.vergara@unisalento.it (D. Vergara), antonio.gaballo@nanotec.cnr.it (A. Gaballo).

[1] Co-first authors.

Alterations in cellular location and expression of E-cadherin are frequently observed in several human diseases. For example, during cancer progression the expression of E-cadherin is lost with a concomitant progression towards a malignant phenotype.[2] This can be mediated in different ways: i) mutational inactivation of *CDH1*; ii) hypermethylation of the DNA encoding E-cadherin; iii) repression by transcription factors; iv) proteolytic cleavage of the extracellular domain. As a result, cell polarity is lost with the activation of transition processes including the epithelial mesenchymal transition program (EMT).[3] In breast cancer, *CDH1* gene is frequently mutated with a complete loss of E-cadherin expression in infiltrating lobular carcinoma[4] and lobular carcinoma *in situ*,[5] but not in ductal tumors.[4] In the absence of inactivating mutations, the expression of E-cadherin at the plasma membrane can be lost due to a process of proteolytic cleavage leading to the release of a soluble extracellular portion of 80 kDa with oncogenic functions.[6] This cleaved fragment shows a correlation with several clinical parameters. For example, soluble E-cadherin (sEcad) levels in breast cancer patients were higher than those of control samples and significantly correlated with tumor/node/metastasis (TNM) stage, tumor grade, and lymph node metastasis.[7] Soluble E-cadherin levels may also predict response after preoperative systemic chemotherapy for patients with breast cancer.[8] Quantitative analysis of sEcad is therefore useful in the clinical setting.

In this context, Surface Plasmon Resonance (SPR) biosensors represent a very powerful approach that is widely reported in the literature for the label-free detection of compounds of clinic interest,[9,10] as well as pollutants or others.[11-13] SPR biosensors have the great advantage to be characterized by high sensitivity that allows the detection of traces of analytes even in complex media. The optical reflectivity of the plasmonic metal, typically gold or silver, is very sensitive to small dielectric changes in the environment in contact to the active layer,[12,14] such as the interaction with the target compound. Furthermore, SPR sensors are often coupled with Quartz Crystal Microbalances (QCMs), gravimetric sensors, to develop selective and sensitive biosensing systems.[15] In this paper, we designed a label-free SPR based approach to accurately detect the soluble form of E-cadherin in sera. It employs a protein A strategy to immobilize anti-E-cadherin antibody (Ab) onto a specific chemically modified substrate. The developed Ab immobilization strategy produces a stable layer that enables the specific detection of soluble E-cadherin as revealed by QCM with Dissipation monitoring (QCM-D) combined with Water Contact Angle (WCA) and Atomic Force Microscopy (AFM) studies. The bioanalytical performance of the developed SPR system was then validated and compared to that of a commercialized ELISA kit using secretomes of breast cancer models and serum clinical samples. The obtained results demonstrated that our SPR-based immunoassay is promising for producing high sensitive and fast response SPR biosensors for cancer diagnosis.

Methods

Cell culture and vectors

Human tumor cells were cultured as described in the Supplementary Methods section and as previously described.[16,17]

Gold substrates functionalization

Before each experiment, gold (Au/mica) substrates for WCA and AFM were cleaned with ultrapure water and ethanol, and functionalized using the MUA/NHS/EDC procedure.[18] Briefly, the gold substrate was immersed overnight into a 10 mM ethanol solution of mercaptoundecanoid acid (MUA) in order to obtain the thiol self-assembled monolayer (SAM). After rinsing, the crystal was incubated for 3 h into a mixture of 15 mM N-hydroxysuccimide (NHS) and 75 mM N- (3-Dimethylaminopropyl)-N-ethylcarbodiimide hydrochloride (EDC) for activation of carboxyl groups. After washing with water and a phosphate buffer solution (PBS), the substrate was immersed into a PBS solution of protein A (protA, 1 μg/mL) for 2 h. After washing with PBS, the sample was incubated into ethanolamine (EA) 1 M in PBS for 10 min and washed again in PBS. Then, gold surfaces have been incubated into 0.2, 1, 2 μg/mL concentration of specific Ab in PBS for two hours. The sample incubated with the highest antibody concentration (2 μg/mL) was immersed in an E- cadherin solution (2 μg/mL in PBS) for 2 h.

QCM experiments

Two different types of QCM sensors were prepared with the aim of a) estimating the Ab coverage (QCM-Ab) and b) defining the E-cadherin range of surface saturation (QCM-Ecad) in the view of optimizing the bonding conditions for SPR assays for E-cadherin fine detection.

QCM-Ab experiments. The sensor was functionalized *ex-situ* following the procedure described above up to the EA step, inserted into the QCM chamber, and conditioned with PBS. After acquiring a reliable baseline for 30 min at 14.1 μl/m, the sensor surface was incubated for 2 h with an anti-Ecad Ab (2 μg/mL). To remove the unreacted Abs, sensor was washed with PBS for 30 min at 40 μl/m.

QCM-Ecad experiments. The sensor was functionalized *ex-situ* following the procedure described above up to the Ab step at 2 μg/mL, inserted into the QCM chamber and conditioned with PBS. After acquiring a reliable baseline for 10 min at 14.1 μl/m, the sensor surface was incubated for 2 h with E-cadherin (0.1, 0.5, 1 and 2 μg/mL). This was followed by a washing step with PBS for 40 min at 30 μl/m to remove the unreacted protein. As control experiment, QCM-Ecad experiment was performed using a sensor functionalized with isotype control Ab flowing E-cad at 2 μg/mL.

QCM measurements were performed using the Q-Sense E1 system (Q-Sense, Sweden), as described elsewhere[19] and in the Supplementary Methods section.

Surface Plasmon Resonance (SPR) measurements

A Nanofilm apparatus was used to perform SPR measurements[20] as described in the Supplementary Methods section.

Results

Soluble E-cadherin levels in breast cancer samples

To determine the soluble levels of E-cadherin in breast cancer samples and to determine whether alterations of the E-cadherin

protein complex might alter the secretome profile, we cultured breast cancer cell lines in serum-free medium, collected sera from a cohort of breast cancer patients and determined levels of soluble E-cadherin by western blot and ELISA.

In luminal epithelial breast cancer cells, E-cadherin is part of a protein complex that plays a role in establishing cell–cell adhesions (Figure 1, *A*). Both E-cadherin and its binding proteins are differentially expressed in luminal and triple negative models where the expression of E-cadherin is transcriptionally down-regulated by promoter methylation (Figure 1, *A*),[21] it is less clear if these differences are maintained in the secretomes of these cell lines. Notably, as demonstrated by western blot, the proteomic signature that is observed at the cellular level is confirmed in the secretome of MCF-7 and MDA-231 cells that were subjected to serum-deprivation for 4 h (Figure 1, *A* and Supplementary Figure 1). At this time point, sEcad is already detectable by western blot with a negligible signal from cytoskeletal intracellular proteins (Supplementary Figure 1, *B*). Thus, E-cadherin complex proteins expression at the secretome level well mirrors the observed cellular differences. In this way, loss of E-cadherin has two main effects that regard the organization of protein complex at the cellular membrane, and the expression of soluble markers in biological fluids. To further investigate this, we stably transfected MCF-7 with an E-cadherin shRNA plasmid (shEcad) and determined by western blot the expression of E-cadherin complex proteins in whole cell lysates and secretomes (Figure 1, *B*). Interestingly, shEcad cells showed a clear modulation in the expression of E-cadherin complex proteins both in whole cell lysates as well as in the secretomes. We quantified sEcad levels by a commercialized ELISA kit (Figure 1, *C*). Compared to control cells, sEcad levels were significantly lower in shEcad cells after 4 h and 24 h of serum-deprivation, providing an evidence of the time-dependent release of the marker in the secretome, and further highlighting the correlation between E-cadherin at the cellular and secretome levels.

ELISA assay was then applied to a panel of luminal breast cancer models (Figure 2, *A*, *B*) and to a cohort of seven serum samples from breast cancer patients and seven control samples (Figure 2, *C*). Significant levels of sEcad were detected in the secretomes of breast cancer cells and quantified in much larger amounts by tumor cells with a higher expression of cellular E-cadherin (Figure 2, *B*). Finally, ELISA results show that the mean level of sEcad is increased in breast cancer compared to the normal controls (Figure 2, *C*). Mean concentrations for soluble E-cadherin in cancer group *vs* control group were 1420 ± 762 ng/mL *vs* 597 ± 390 ng/mL, respectively.

Design, optimization, and application of the SPR-based immunoassay for biological samples

The stable functionalization of the surface sensor is an essential step for a sensitive detection of E-cadherin at low concentration. To do this, the anti-Ecad Ab that we validated by western blot using the secretomes of breast models was covalently attached onto a gold surface. On the basis of the well-known thiol-chemistry,[22] we produced a compact SAM ofMUA that was activated to promote protA attachment *via* amidebond. The un-reacted sites were blocked using EA. ProtA has the capability to bind antibodies at the Fc region[23] so to force its orientation on the surface leaving free the portion that reacts with soluble E-cadherin. We applied a combination of techniques to optimize the Ab coverage on the sensor surface: a) WCA, b) AFM, c) QCM and FT-IR spectroscopy. WCA and QCM allowed to quickly monitor each step of functionalization and to screen the concentration corresponding to a high and uniform coverage of Ab. QCM was used to estimate the Ab surface coverage and to establish the optimal conditions for the detection of soluble E-cadherin in secretomes and serum samples. As WCA values reported in Table 1 show, the addition of protA to aMUA SAM increases the surface hydrophobicity, because the carboxylic groups of the SAM have been replaced by EA and by the proteins that probably expose more hydrophobic domains. The addition of Ab at growing concentrations (0.2, 1, 2 μg/mL) determines a progressively increase of hydrophilicity of the surface (46.75° ± 0.53° at 0.2 μg/mL and 37.88° ± 1.68° at 1 μg/mL) that reaches its maximum (WCA drops to 0°) for 2 μg/mL solution of Ab. WCA variations are associated to an increase of the surface roughness as calculated by AFM measurements (Table 1 and Supplementary Figure 2). This is expected considering that several molecular layers were assembled on the sensor surface. AFM measurements were also used to estimate the Ab surface coverage in combination with QCM measurements (QCM-Ab experiments described above). Assuming the overestimation that is related to tip effects, we calculated a single Ab diameter of 25 ± 5 nm, a value that is consistent with previous AFM experiments.[24]

Figure 3, *A* represents the QCM spectrum acquired to quantify the amount of antibody bond to the sensor surface after 2 h of incubation with a solution of 2 μg/mL. After the stabilization in pure PBS, the Ab solution was flowed into the QCM chamber for 25 min and allowed to react for two hours stopping the flow (area of red diagonal stripes in Figure 3, *A*). A frequency signal was observed after 10 min from the Ab injection, indicating a mass increase. The process occurring at the sensor–liquid interface is sketched as inset of Figure 3, *A*. After rinsing with PBS flow, only covalently attached antibodies persisted on the surface. The specificity of protA anti-Ecad Ab binding was confirmed by FT-IR spectroscopy analysis. FT-IR spectra are reported in Figure 3, *B*. The successful functionalization by anti-Ecad Ab molecules was confirmed comparing the spectrum of the multi-layer film obtained after the binding of the Ab at a concentration 2 μg/ml (Figure 3, *B*, curve ii) to the FT-IR spectra of cast film of protA and anti-Ecad Ab onto gold substrates (Figure 3, *B*, line i and iii, respectively). All the FT-IR spectra are reported in the 1800-1400 cm^{-1} frequency range in order to observe Amide I and II contributes, which can be considered as marker bands for protein characterization[25] and are due to C=O stretching mode and N-H bending mode of the amide group.[26] Any protein presents its own Amide I/Amide II profile and such features were used to confirm the presence of each molecular layer in the developed multi-layer system, namely protA, anti-Ecad Ab and, finally, the bonded E-cadherin. ProtA Amide II has a characteristic signal located at about 1544 cm^{-1} (highlighted in red), with Ab at 1596 cm^{-1} (blue highlighted). The spectrum of the functionalized film (Figure 3, *B*, line ii) is characterized by the presence of such signals confirming the binding of anti-Ecad Ab molecules to the protA layer. Moreover, the Amide I (at about 1650 cm^{-1})/Amide II (at about

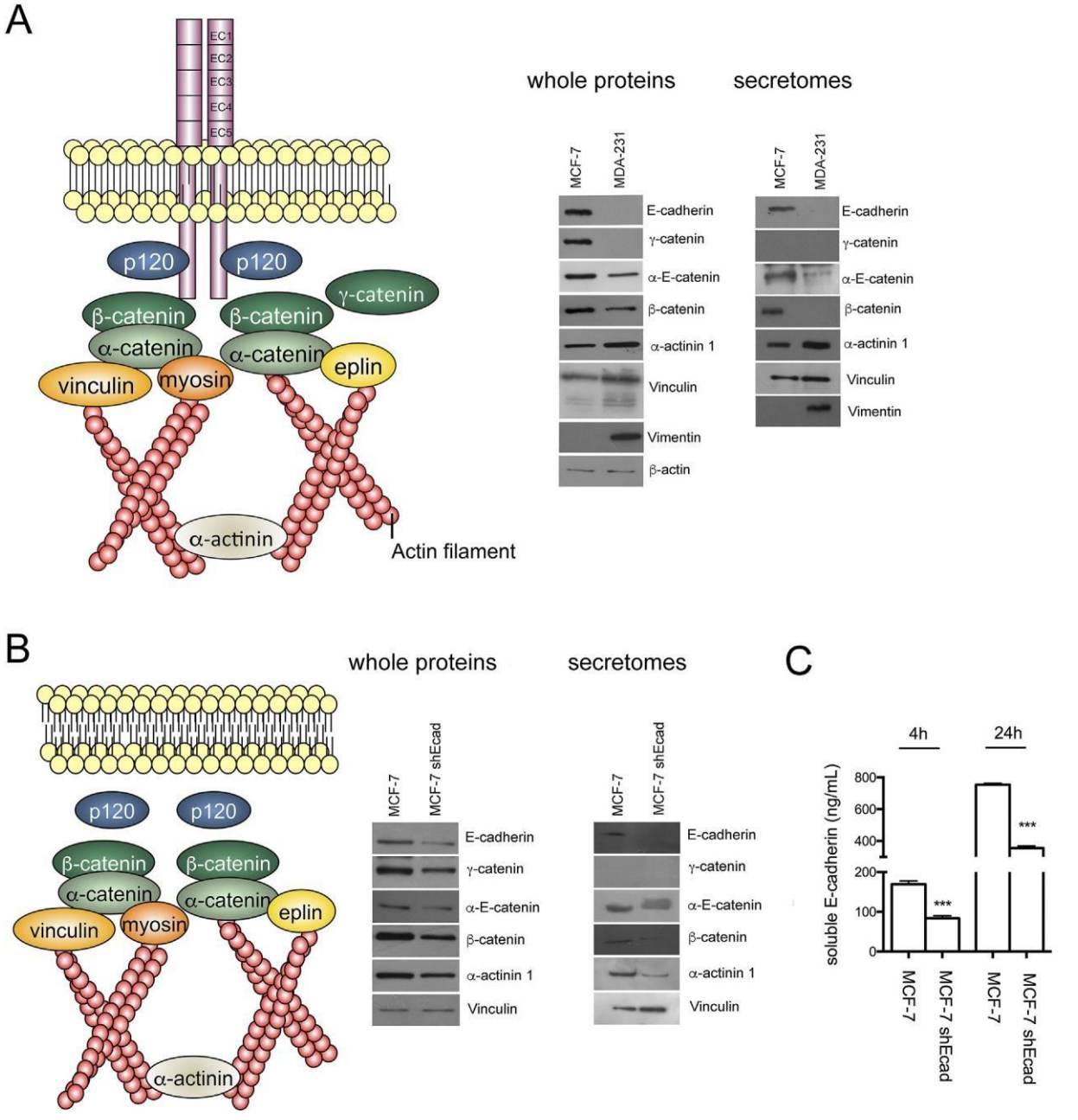

Figure 1. Differential expression of E-cadherin complex proteins in breast cancer models. (A) Representative image of the E-cadherin complex at the plasma membrane. Through its intracellular domain, E-cadherin interacts with β-catenin and other proteins that in turn bind with the cytoskeleton. Western blot of selected proteins was performed on whole proteins and secretomes of MCF-7 and MDA-231 cells. (B) Western blot of selected proteins was performed on whole proteins and secretomes of MCF-7 and MCF-7 shEcad cells. (C) Soluble E-cadherin levels (ng/mL) measured by ELISA in the secretomes of MCF-7 and MCF-7 shEcad cells after 4 h and 24 h of growth in a medium without serum. Data are mean ± SD of three independent experiments. *** P b 0.001.

1596 cm^{-1}) intensity band ratio is clearly comparable to such a ratio obtained for the anti-Ecad Ab cast film (curve iii).

QCM experiments were then performed to determine the binding efficiency of the Ab monolayer and the maximum protein coverage (1:1 Ab:Ecad ratio). To do this, we injected into the QCM chamber four solutions of E-cadherin at different concentrations, using a sensor with an Ab concentration of 2 μg/mL (QCM-Ecad experiments described above). After an initial stabilization in PBS, the E-cadherin solution was flowed and allowed to react for two hours after stopping the flow (area of red diagonal stripes in Figure 3, *C*). After this step, the surface sensor was fluxed with PBS to wash away the un-reacted E-cadherin, while the bound protein was quantified. To verify the detection specificity of our Ab, QCM experiments were performed in the same experimental conditions using a non-specific antibody (isotype control). After the initial adsorption step, PBS was fluxed and a large amount of adsorbed E-cad was washed away (Figure 3, *C*, red curve). This indicates that the

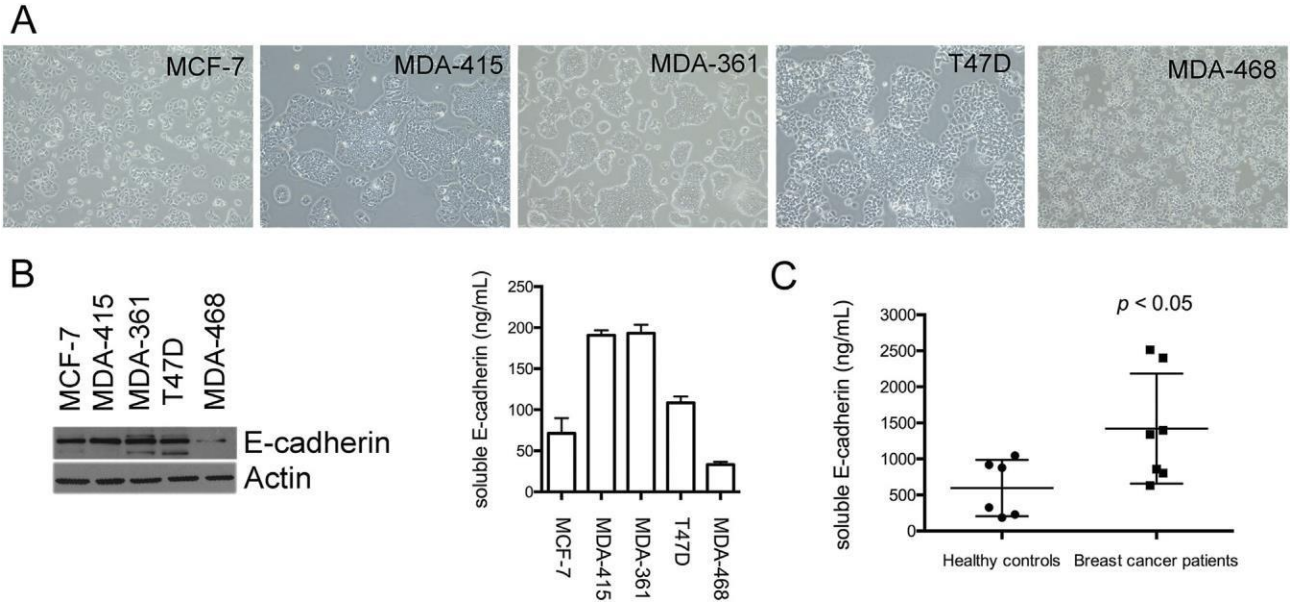

Figure 2. Soluble E-cadherin levels in the secretomes and serum of breast cancer samples. (A) Phase contrast images of epithelial breast cancer cell lines (Olympus IX51 inverted microscope, 4× magnification). (B) Levels of cellular E-cadherin and soluble E-cadherin in whole cell lysates and secretomes as determined by western blot and ELISA data, respectively. Actin was used as loading control. ELISA data are mean ± SD of three independent experiments. (C) Levels of soluble E-cadherin in serum as determined by ELISA. Serum samples from 7 control samples were compared to the levels of E-cadherin in 7 patients with breast cancer. The horizontal long line in each dot blots indicates the mean, while the top and bottom shorter lines mark the standard deviation. *P* value was calculated by Mann–Whitney test.

Table 1

Rq (root mean square) roughness as calculated from AFM images of Supplementary Figure 2 and WCA values for samples at different functionalization steps.

	MUA	MUA/protA/EA	MUA/protA/EA/Ab	MUA/protA/EA/Ab/E-cad
Rq (nm)	0.25 ± 0.02	0.50 ± 0.09	0.69 ± 0.14	1.52 ± 0.18
WCA (°)	47.64 ± 2.16	50.53 ± 0.34	0	52.57 ± 1.36

selected Ab is able to maximize the interaction with E-cad and demonstrates the selectivity of the developed immunoassay for E-cad specific molecular recognition. These experimental evidences represented the starting point for the development of the SPR based transduction system.

The E-cadherin binding on the sensor was further confirmed by FT-IR spectroscopy analysis. The spectrum of the multi-layer sensor after E-cadherin binding within the QCM cell was recorded and shown in Figure 3, *D* (black spectrum). By comparing this spectrum to the E-cadherin cast film onto gold substrate spectrum (Figure 3, *D*, gray spectrum), the presence of E-cad was assessed due to specific interaction among the antigen and the Ab. In fact, the Amide I band, in the range 1690- 1650 cm^{-1}, resulted affected by the binding with Ecad, as highlighted in Figure 3, *D*, with an evident contribute located atabout 1680 cm^{-1}, ascribable to the Ecad Amide I. Furthermore,the signal at 1510 cm^{-1}, typical of Ecad molecules, is present inthe spectrum of the film after the interaction with the antigen. Notably, the peaks arising from protA and anti-Ecad Ab (highlighted in red in the Figure 3, *D*) are still noticeable in the spectrum, underlining that the molecular architecture of the sensor is stable under the tested conditions.

The optimized protocol was indeed exploited to develop an SPR-based assay for the detection of E-cadherin in biological fluids like secretome and sera. A schematic representation of the SPR based system used is reported in Figure 4, *A*. In order to calculate the concentration of Ecad in the investigated biological samples, we determined a calibration curve, SPR angle shift (Δ_{AOI}) *vs* Ecad concentration (Figure 4, *C*). The Δ_{AOI} was obtained by measuring the SPR angle when the multi-layer film was exposed to a DMEM flux (2 mL as total DMEM volume fluxed during the calibration) for 90 min (AOI_i), then by inducing the Ecad binding fluxing protein solutions (in DMEM) at known concentration within the cell for 90 min, and, finally, measuring the SPR angle of the washing step, fluxing a fresh DMEM solution for 90 min (AOI_f), in order to remove eventual non-specific adsorptions. The Δ_{AOI} was calculated as $AOI_i - AOI_f$. In particular, the response of the multi-layer system was investigated by fluxing different E-cad concentrations (50, 100, 200, 370 and 500 ng/mL). A dynamic response was recorded in the investigated range. Nonetheless, a linear correlation between Δ_{AOI} and Ecad concentration (ng/mL) could be found by fixing the working concentration range between 0 and 200 ng/mL (Figure 4, *C*). SPR curves obtained for each investigated Ecad concentrations in DMEM

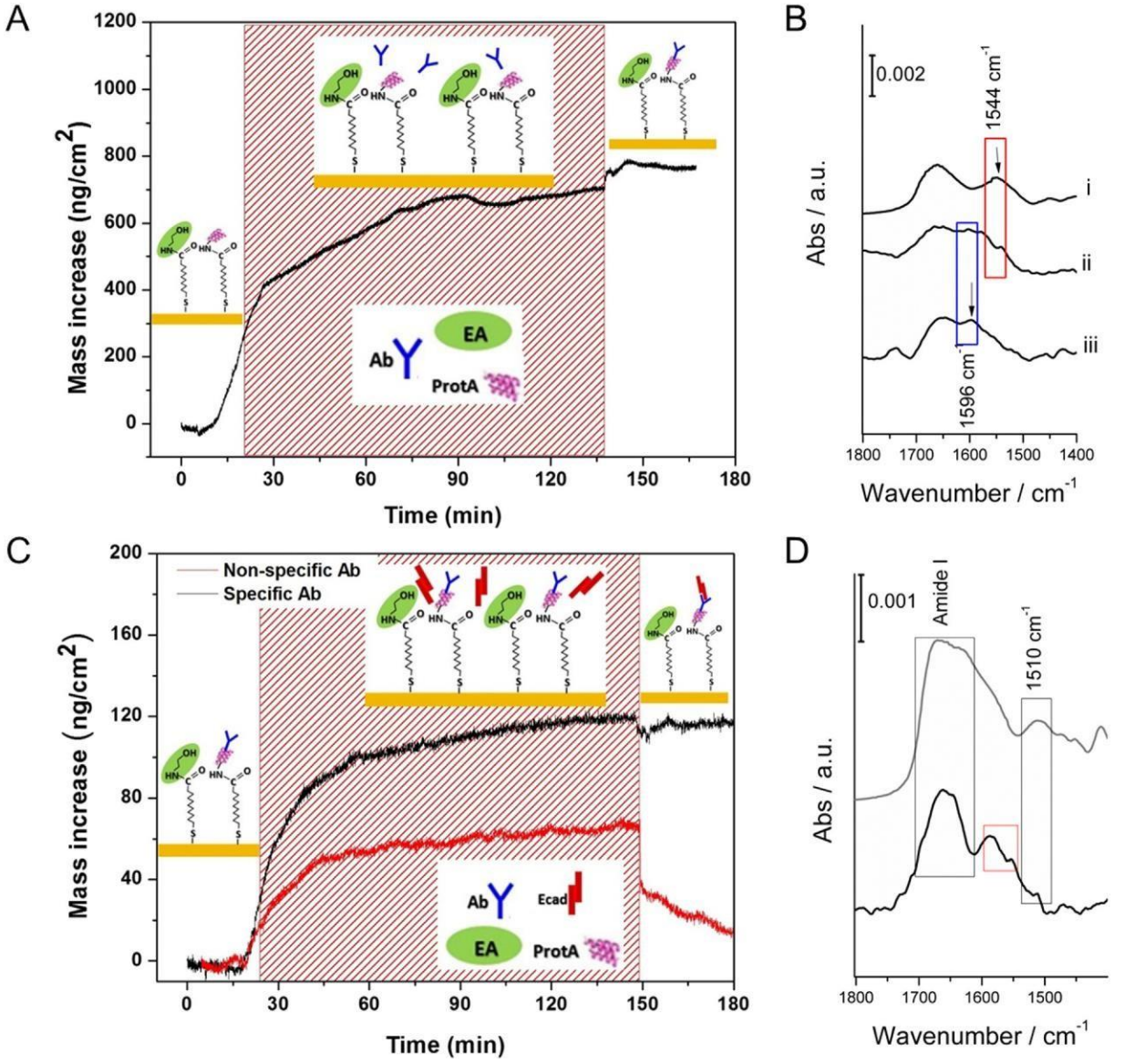

Figure 3. QCM analysis of soluble Ecad. (A) QCM spectrum of a sensor functionalized *ex-situ* with MUA/protA/EA and treated with a 2 μg/mL solution of Ab. After flowing PBS for 10 min, the Ab solution was added and allowed to react for 2 h. The red panel represents the incubation step followed by a washing step in PBS. Inset: sketch of the surface steps of functionalization. (B) FT-IR spectra of (i) cast film of protA onto gold substrate, (ii) dried multi-layered film obtainedby using a solution 2 mg/mL of anti-Ecad Ab and (iii) cast film of anti-Ecad Ab onto gold substrate, 1800-1400 cm^{-1} range. (C) QCM spectrum of a sensor functionalized *ex-situ* with MUA/protA/EA/Ab and treated with a 2 μg/mL solution of E-cad. After flowing PBS for 10 min, E-cad solution was added and allowed to react for 2 h. The red panel represents the incubation step followed by a washing step in PBS. The black curve was acquired using a sensor functionalized with a specific Ab. The red curve was acquired using a sensor functionalized with a non-specific Ab. Inset: sketch of the surface steps of functionalization. (D) FT-IR spectra of a cast film of Ecad onto gold substrate (gray spectrum) and dried multi-layered film treated with Ecad (black spectrum) within the QCM cell in the 1800-1400 cm^{-1} range.

(50, 100, 200, 370 and 500 ng/mL) are reported in Figure 4, *B*. It is evident that the Δ_{AOI} increases as the Ecad solution concentration increases as well, until the reaching of a plateau phase, after 200 ng/ml Ecad solution fluxing, where to E-cad concentration change corresponds very small AOI shift, due to presumable active sites saturation. FT-IR spectroscopy was also carried out to confirm the binding of E-cad molecules (Figure 4, *D*).

In the spectrum obtained after the binding (Figure 4, *D*, line e), the signals at about 1680 cm^{-1} and 1660 cm^{-1}, attributed to the C=O stretching mode of the Amide I of Ecad (squared in Figure 4, *D*, line e and f), and the signal at 1510 cm^{-1} related to the Ecad backbone vibration mode are well-visible.

The developed multi-layer system was then tested for the detection and quantification of Ecad levels present in the secretome of MCF-7 cells after 4 h of starvation. The amount of Ecad was calculated by using the calibration curve shown in Figure 4, *B*. The Δ_{AOI} was obtained as the difference between the SPR angle measured when a DMEM (2 mL) solution was fluxed within the cell (Supplementary Figure 4, *A*, black line), and the SPR angle measured by fluxing a DMEM solution after that the

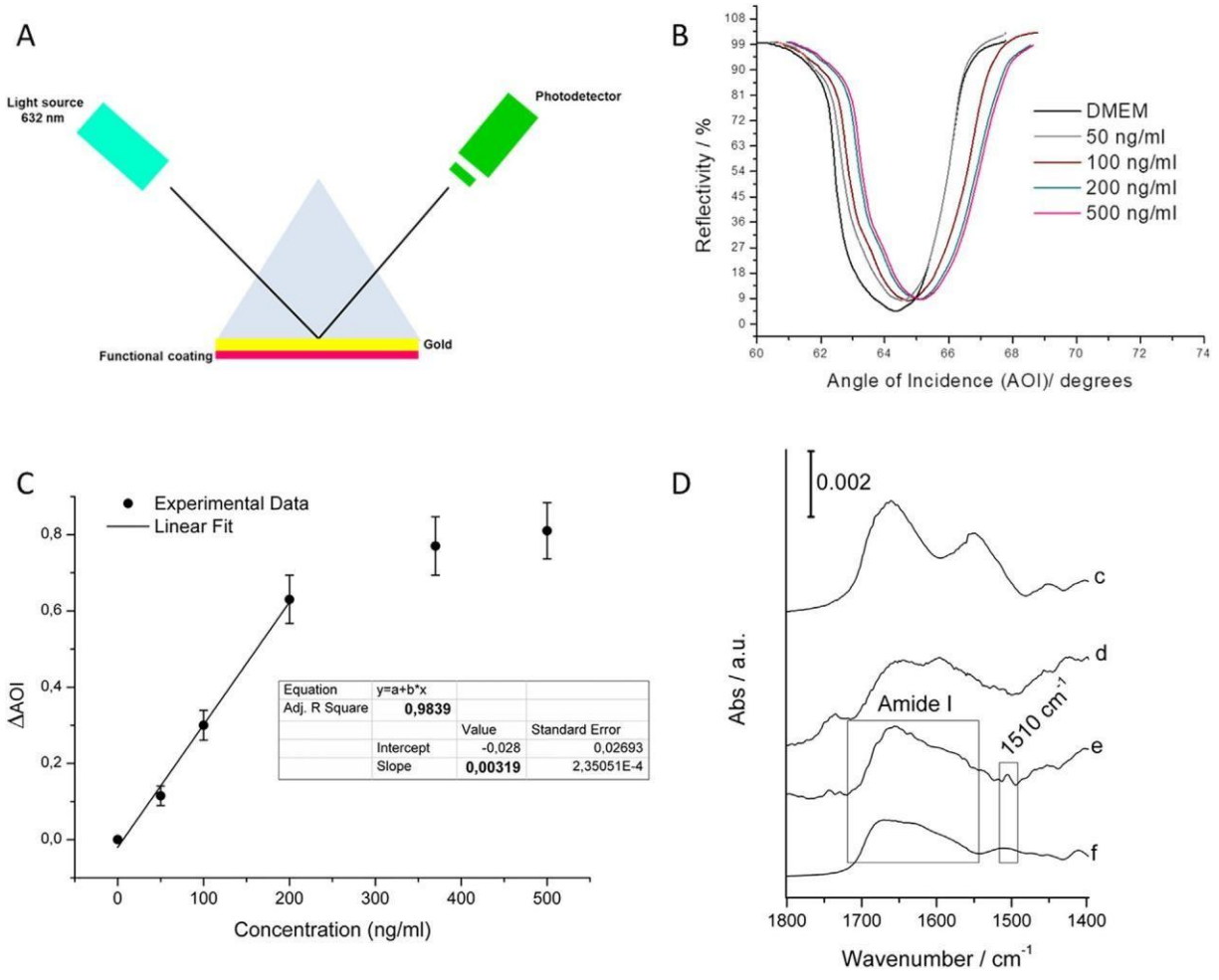

Figure 4. SPR analysis of soluble Ecad. (A) Schematization of the SPR system (Kretschmann configuration). (B) SPR curve for the Au/glass substrate functionalized by the multi-layered film obtained by using a solution 2 μg/ml of anti-Ecad Ab (black line), after fluxing 0.05 μg/mL (gray line), 0.1 μg/mL (red line), 0.2 μg/mL (green line) and 0.5 μg /mL Ecad solution (pink line). (C) calibration curve Δ_{AOI} *vs* Ecad concentration in DMEM solution and the obtained linear fitting in the linear range 0-200 ng/mL. (D) FT-IR spectra of (c) cast film of Protein A onto gold substrate, (d) cast film of anti-Ecad Ab onto gold substrate, (e) dried multi-layered film obtained by using a solution 2 μg/mL of anti-Ecad Ab and treated by fluxing Ecad solution 0.2 mg/mL within the SPR cell and (f) cast film of Ecad onto gold substrate in the 1800-1400 cm^{-1} frequency range.

secretome solution (2 mL) was fluxed for 90 min (Supplementary Figure 4, *A*, gray line). The obtained Δ_{AOI} was calculated to be 0.19 and by data interpolation on the calibration line, we determined a concentration of Ecad in the secretome of 59.56 ± 10.34 ng/mL that is in good agreement with data obtained by ELISA (Figure 2, *B*).

Finally, two clinical samples were analyzed using the SPR sensor (Supplementary Figure 4, *B* and inset). Δ_{AOI} was calculated as the difference between the SPR angle measured when a solution of DMEM (2 mL) was fluxed on the film, and the SPR angle measured by fluxing a fresh DMEM solution after that the sensor was exposed for 90 min to the flux of the serum solution. In detail, 0.6 mL and 0.08 mL of control and patient serum were diluted in DMEM to a final volume of 2 mL. After DMEM washing, we measured an SPR shift of 0.29 for the control and 0.31 for the patient and we calculated a concentration of Ecad of 90.90 ± 15.78 ng/mL and 97.17 ± 16.86 ng/mL. These values were multiplied for the dilution factor of each sample to obtain a concentration of 300 ± 52.07 ng/mL for the control and 2420 ± 419.7 ng/mL for the patient serum, in good agreement with ELISA (314 ± 24.7 ng/mL and 2390 ± 192.7 ng/mL, respectively).

Discussion

The EMT process has a central role in physiological and pathological conditions. During cancer progression, EMT promotes invasion and confers tumor cells with stem cell-like properties.[27] Recent data from different tumor types have defined a set of biological networks and pathways modified during EMT.[28,29] This includes also a long list of biomarkers including proteins, nucleic acids, and lipids that demonstrated a robust clinical validity.[3,30] If these biomarkers showed diagnostic or prognostic value when their expression is investigated at the tissue level, it is reasonable to propose these as potential circulating markers if released in blood or other biological fluids.

Based on this assumption, we validated the different expression of selected EMT markers in breast cancer models

and investigated their presence in the secretomes of our models. As shown, the classical EMT markers E-cadherin and vimentin well characterized MCF-7 and MDA-231 cells for their epithelial and mesenchymal phenotype, respectively (Figure 1, *A*). By western blot, we confirmed this difference in the secretome of both cell models (Figure 1, *A*). Our hypothesis was subsequently verified at pathway level. Alterations in the organization of cell–cell junction proteins orchestrate the activation of EMT, with important consequences on the expression of these markers at cellular level. As we demonstrated here, when we compared western blot data from the secretomes with that collected from cell lysates, epithelial and mesenchymal breast cancer cells showed a different expression of the protein components of the E-cadherin complex (Figure 1, *A*). Similar findings were described for the secretome of MCF-7 and MCF-7 shEcadcells. Down-regulation of E-cadherin induced changes in the expression of E-cadherin complex proteins at cellular level with a consequent reduction of their secreted levels (Figure 1, *B*). This confirms that the secretome is functionally linked to the cell phenotype, and that the release of proteins is a time-dependent process, as demonstrated by ELISA (Figure 1, *C*). With the aim to transfer these biological results in the realization of an SPR-based immunoassay, we decided to focus our attention on E-cadherin. To determine the analytical potential of our system, we determined sEcad level in secretomes and serum samples by ELISA. As shown in Figure 2, *A* and *B*, we selected a panel of epithelial breast cancer models and we determined sEcad levels in their secretomes, and E-cadherin levels in their cellular lysates. Data reported in the histograms describe the sEcad levels detected for each concentrated conditioned media samples after 4 h of serum starvation (Supplementary Figure 1), with a range to less than 50 ng/mL to 200 ng/mL. Serum levels of E-cadherin were significantly higher compared to secretomes, and significantly increased in breast cancer samples (Figure 2, *C*). Overall, these experiments allowed assessing the concentration range of E-cadherin in secretome and serum samples for the development of QCM-sensor and SPR application. To do this, we assembled an E-cadherin sensing layer using different functionalization steps (consisting of MUA/ProtA/EA/Ab). AFM, WCA and FT-IR studies, shown in Figure 3, *B* and Supplementary Figure 2, and the values reported in Table 1 performed at the different functionalization steps, give a clear indication of the multilayer structures assembled on the top of the sensor.

Subsequently, QCM-Ab experiments were performed to calculate the amount of Ab on the top of the functionalized sensors corresponding to 703 ng/cm^2. Considering that from the AFM estimation, the area occupied by a single Ab is 491 nm^2, and that the Ab molecular weight is 150 kDa, we calculated a concentration of immobilized Ab of 4.69×10^{-12} mol cm^{-2}. This corresponds to a sensor surface coverage of 91%, which means that a homogeneous distribution of Ab molecules has been achieved using the proposed functionalization method.

QCM data reported in Supplementary Figure 3, permitted to determine a correlation between the levels of Ecad in solution and those adsorbed onto the sensor surface. When the sensor was incubated with a solution of Ecad concentrated at 2 μg/mL, 113.02 ± 4.63 ng/cm^2 of protein was immobilized. A linear trend was observed with a slope of 51.98 ± 3.61 μL/cm^2. If the sensor surfaces were saturated, a concentration of $4{,}69 \times 10^{-12}$ mol cm^{-2} should be present. The weight of Ecad calculated *via* QCM would be of 281 ng/cm^2 corresponding to a solution of 5.4 μg/mL, which represents the highest Ecad concentration that can be measured using the optimized functionalization. This is the range of soluble Ecad concentration described in several studies or public databases (http://www.plasmaproteomedatabase.org/). Therefore, this preliminary study demonstrates that the developed functionalization is efficient enough to allow the detection of E-cad in sera without the risk to saturate the active sites. As further result, FT-IR spectra of Figure 3, *D* confirm that the mass increase, registered by QCM, is due to the bond of E-cad to the sensing layer. All these experimental evidences were exploited to develop a SPR system, tested for the detection of E-cadherin into DMEM, cells secretome and human sera. Even in this case, FT-IR spectroscopy characterization was used to ensure the functionalization and E-cadherin binding, allowing the identification of the protein marker bands in the assembled multi-layer. Then, the system response to different concentrations of E-cadherin in DMEM solutions was investigated, showing a dynamic response up to 500 ng/mL of the protein. For this reason, a static range was found between 0 and 200 ng/mL and a calibration linear curve Δ_{AOI} *vs* protein concentration (ng/mL) was obtained and is reported in Figure 4, *C* (correlation coefficient of 0.9839). The limit of detection (LOD) was calculated from the slope of the calibration linear curve and the standard deviation on multiple measurements of the blank sample (n = 5), as previously described[31,32]:

$$LOD = \frac{\sigma \omega F}{b}$$

where σ is the standard deviation of the blank sample, F is a factor of 3.3 and b is the slope of the regression line. A LOD of 16 ± 6.5 ng/mL of E-cadherin was found, corresponding to a concentration of about 200 pmol that is 6 times higher than the LOD of the employed ELISA test (100 ng/mL; ~1.25 nmol). The analytical sensitivity was calculated by the ratio of the amount of detected protein (ng/mL) and the Δ_{AOI} (degrees) correspondent, and was found to be 300 (ng/ml)/°. Overall, this highlights the feasibility of our system in the detection of tissue leakage markers whose concentration in plasma ranges from 10^6 to 10^2 pg/mL.[33] The attractiveness of this method relies also in the absence of pre-concentration step as we determined Ecad in serum using only few μl of sample. Sensitivity should be further improved to characterize signal proteins such as cytokines and growth factors and this is a common issue for SPR detection of protein in biological fluids.[34–36] In this direction, a possible approach, widely employed in the literature, could be based on the amplification of the signal by introducing colloidal gold nanoparticles[37,38] or plasmon metal nanostructures,[39,40] allowing a detection down to femtomolar amount of proteins.

Acknowledgment

We thank Dr. Roberto Rella and Dr. Maria Grazia Manera for the preparation of the SPR supports and for the important discussion about SPR measurements.

Appendix A. Supplementary data

Supplementary data to this article can be found online.

References

1. Shapiro L, Weis WI. Structure and biochemistry of cadherins and catenins. *Cold Spring Harb Perspect Biol* 2009;1a003053.
2. Jeanes A, Gottardi CJ, Yap AS. Cadherins and cancer: how does cadherin dysfunction promote tumor progression? *Oncogene* 2008;27:6920-9.
3. Vergara D, Simeone P, Frank J, Trerotola M, Giudetti A, Capobianco L, et al. Translating epithelial mesenchymal transition markers into the clinic: novel insights from proteomics. *EuPA Open Proteom* 2016;10:31-41.
4. Ciriello G, Gatza ML, Beck AH, Wilkerson MD, Rhie SK, Pastore A, et al. Comprehensive molecular portraits of invasive lobular breast cancer. *Cell* 2015;163:506-19.
5. McCart Reed AE, Kutasovic JR, Lakhani SR, Simpson PT. Invasive lobular carcinoma of the breast: morphology, biomarkers and 'omics. *Breast Cancer Res* 2015;17:12.
6. David JM, Rajasekaran AK. Dishonorable discharge: the oncogenic roles of cleaved E-cadherin fragments. *Cancer Res* 2012;72:2917-23.
7. Liang Z, Sun XY, Xu LC, Fu RZ. Abnormal expression of serum soluble E-cadherin is correlated with clinicopathological features and prognosis of breast cancer. *Med Sci Monit* 2014;20:2776-82.
8. Hofmann G, Balic M, Dandachi N, Resel M, Schippinger W, Regitnig P, et al. The predictive value of serum soluble E-cadherin levels in breast cancer patients undergoing preoperative systemic chemotherapy. *Clin Biochem* 2013;46:1585-9.
9. Masson JF. Surface plasmon resonance clinical biosensors for medical diagnostics. *ACS Sens* 2017;2:16-30.
10. Wang W, Mai Z, Chen Y, Wang J, Li L, Su Q, et al. A label-free fiber optic SPR biosensor for specific detection of C-reactive protein. *Sci Rep* 2017;7:16904.
11. Arora P, Sindhu A, Dilbaghi N, Chaudhury A. Biosensors as innovative tools for the detection of food borne pathogens. *Biosens Bioelectron* 2011;28:1-12.
12. Li Y, Zhu J, Zhang H, Liu W, Ge J, Wu J, et al. High sensitivity gram-negative bacteria biosensor based on a small-molecule modified surface plasmon resonance chip studied using a laser scanning confocal imaging-surface plasmon resonance system. *Sens Actuators B* 2018;259:492-7.
13. Milanese M, Ricciardi A, Manera MG, Colombelli A, Montagna G, de Risi A, et al. Real time oil control by surface plasmon resonance transduction methodology. *Sensors Actuators A Phys* 2015;223:97-104.
14. Guo X. Surface plasmon resonance based biosensor technique: a review. *J Biophotonics* 2012;5:483-501.
15. Sun W, Song W, Guo X, Wang Z. Ultrasensitive detection of nucleic acids and proteins using quartz crystal microbalance and surface plasmon resonance sensors based on target-triggering multiple signal amplification strategy. *Anal Chim Acta* 2017;978:42-7.
16. Onder TT, Gupta PB, Mani SA, Yang J, Lander ES, Weinberg RA. Loss of E-cadherin promotes metastasis via multiple downstream transcriptional pathways. *Cancer Res* 2008;68:3645-54.
17. Vergara D, Simeone P, Latorre D, Cascione F, Leporatti S, Trerotola M, et al. Proteomics analysis of E-cadherin knockdown in epithelial breast cancer cells. *J Biotechnol* 2015;202:3-11.
18. Bianco M, Aloisi A, Arima V, Capello M, Ferri-Borgogno S, Novelli F, et al. Quartz crystal microbalance with dissipation (QCM-D) as tool to exploit antigen-antibody interactions in pancreatic ductal adenocarcinomadetection. *Biosens Bioelectron* 2013;42:646-52.
19. Rodahl M, Hook F, Krozer A, Brzezinski P, Kasemo B. Quartz-crystal microbalance set up for frequency and Q-factor measurements in gaseous and liquid environments. *Rev Sci Instrum* 1995;66:3924-30.
20. Bettini S, Maglie E, Pagano R, Borovkov V, Inoue Y, Valli L, et al. Conformational switching of ethano-bridged cu,H2-bis-porphyrin induced by aromatic amines. *Beilstein J Nanotechnol* 2015;6:2154-60.
21. Lombaerts M, van Wezel T, Philippo K, Dierssen JW, Zimmerman RM, Oosting J, et al. E-cadherin transcriptional downregulation by promoter methylation but not mutation is related to epithelial-to- mesenchymal transition in breast cancer cell lines. *Br J Cancer* 2006;94:661-71.
22. Arima V, Blyth RIR, Della Sala F, Del Sole R, Matino F, Mele G, et al. Long-range order induced by cobalt porphyrin adsorption on aminothiophenol-functionalized au(111): the influence of the induced dipole. *Mater Sci Eng C* 2004;24:569-73.
23. Choe W, Durgannavar TA, Chung SJ. *Fc-Binding Ligands of Immunoglobulin G: An Overview of High Affinity Proteins and Peptides*,9; 20161-17.
24. Tan YH, Liu M, Nolting B, Go JG, Gervay-Hague J, Liu GY. A nanoengineering approach for investigation and regulation of protein immobilization. *ACS Nano* 2008;2:2374-84.
25. Terzi A, Storelli E, Bettini S, Sibillano T, Altamura D, Salvatore L, et al. Effects of processing on structural, mechanical and biological properties of collagen-based substrates for regenerative medicine. *Sci Rep* 2018;8:1429.
26. Silverstein RM, Bassler GC, Terence CM. fourth edition. *Spectrometric identification of organic compounds*. John Wiley & Sons Edition; 1981. p. 95-180.
27. Shibue T, Weinberg RA. EMT, CSCs, and drug resistance: the mechanistic link and clinical implications. *Nat Rev Clin Oncol* 2017;14:611-29.
28. De Domenico S, Vergara D. The many-faced program of epithelial-mesenchymal transition: a system biology-based view. *Front Oncol* 2017;7:274.
29. Guerra F, Guaragnella N, Arbini AA, Bucci C, Giannattasio S, Moro L. Mitochondrial dysfunction: a novel potential driver of epithelial-to-mesenchymal transition in cancer. *Front Oncol* 2017;7:295.
30. Santamaria PG, Moreno-Bueno G, Portillo F, Cano A. EMT: present and future in clinical oncology. *Mol Oncol* 2017;11:718-38.
31. Bianco M, Sonato A, De Girolamo A, Pascale M, Romanato F, Rinaldi R, et al. An aptamer-based SPR-polarization platform for high sensitive OTA detection. *Sensors Actuators B Chem* 2017;241:314-20.
32. Shrivastava A, Gupta V. Methods for the determination of limit of detection and limit of quantitation of the analytical methods. *Chron Young Sci* 2011;2:21-5.
33. Geyer PE, Holdt LM, Teupser D, Mann M. Revisiting biomarker discovery by plasma proteomics. *Mol Syst Biol* 2017;13:942.
34. Li G, Li X, Yang M, Chen MM, Chen LC, Xiong XL. A gold nanoparticles enhanced surface plasmon resonance immunosensor for highly sensitive detection of ischemia-modified albumin. *Sensors (Basel)* 2013;13:12794-803.
35. Huang CF, Yao GH, Liang RP, Qiu JD. Graphene oxide and dextran capped gold nanoparticles based surface plasmon resonance sensor for sensitive detection of concanavalin a. *Biosens Bioelectron* 2013;50:305-10.
36. Azzam E, Abd El-aal A, Shekhah O, Arslan H, Wöll C. Fabrication of spr nanosensor using gold nanoparticles and self-assembled monolayer technique for detection of cu2+ in an aqueous solution. *J Dispers Sci Technol* 2013;35:1-7.
37. Kwon MJ, Lee J, Wark AW, Lee HJ. Nanoparticle-enhanced surface plasmon resonance detection of proteins at attomolar concentrations: comparing different nanoparticle shapes and sizes. *Anal Chem* 2012;84:1702-7.
38. Cao Y, Griffith B, Bhomkar P, Wishart DS, McDermott MT. Functionalized gold nanoparticle-enhanced competitive assay for sensitive small-molecule metabolite detection using surface plasmon resonance. *Analyst* 2017;143:289-96.
39. Indutnyi I, Ushenin Y, Hegemann D, Vandenbossche M, Myn'ko V, Lukaniuk M, et al. Enhancing surface plasmon resonance detection using nanostructured au chips. *Nanoscale Res Lett* 2016;11:535.
40. Byun KM, Yoon SJ, Kim D, Kim SJ. Experimental study of sensitivity enhancement in surface plasmon resonance biosensors by use of periodic metallic nanowires. *Opt Lett* 2007;32:1902-4.